BIOMOLECULES & THERAPEUTICS

Original Article
Biomol Ther 32(5), 627-634 (2024)

Unraveling Stereochemical Structure-Activity Relationships of Sesquiterpene Lactones for Inhibitory Effects on STAT3 Activation

Seungchan An[1], Jaemoo Chun[2], Joohee Lee[1,3], Yeong Shik Kim[1], Minsoo Noh[1,*] and Hyejin Ko[1,4,*]

[1]College of Pharmacy, Natural Products Research Institute, Seoul National University, Seoul 08826,
[2]KM Convergence Research Division, Korea Institute of Oriental Medicine, Daejeon 34054,
[3]Department of Dermatology, Severance Hospital, Cutaneous Biology Research Institute, Yonsei University College of Medicine, Seoul 03722,
[4]Natural Products Research Center, Korea Institute of Science and Technology (KIST), Gangneung 25451, Republic of Korea

Abstract

Sesquiterpene lactones, a class of natural compounds abundant in the Asteraceae family, have gained attention owing to their diverse biological activities, and particularly their anti-proliferative effects on human cancer cells. In this study, we systematically investigated the structure-activity relationship of ten sesquiterpene lactones with the aim of elucidating the structural determinants for the STAT3 inhibition governing their anti-proliferative effects. Our findings revealed a significant correlation between the STAT3 inhibitory activity and the anti-proliferative effects of sesquiterpene lactones in MDA-MB-231 breast cancer cell lines. Among the compounds tested, alantolactone and isoalantolactone emerged as the most potent STAT3 inhibitors, highlighting their potential as candidates for anticancer drug development. Through protein-ligand docking studies, we revealed the structural basis of STAT3 inhibition by sesquiterpene lactones, emphasizing the critical role of hydrogen-bonding interactions with key residues, including Arg609, Ser611, Glu612, and Ser613, in the SH2 domain of STAT3. Furthermore, our conformational analysis revealed the decisive role of the torsion angle within the geometry-optimized structures of sesquiterpene lactones in their STAT3 inhibitory activity (R=0.80, p<0.01). These findings not only provide preclinical evidence for sesquiterpene lactones as promising phytomedicines against diseases associated with abnormal STAT3 activation, but also highlight the importance of stereochemical aspects in their activity.

Key Words: Sesquiterpene lactone, STAT3, Alantolactone, Protein-ligand docking, Torsion angle, Stereochemical structure-activity relationship

INTRODUCTION

Sesquiterpene lactones, plant secondary metabolites belonging to the terpenoid class, are distinctive constituents of the Asteraceae family (Hristozov *et al*., 2007; Shulha and Zidorn, 2019; Dhyani *et al*., 2022). These compounds exhibit a remarkable spectrum of biological activities, including anti-proliferative, anti-inflammatory, and anti-microbial effects (Matos *et al*., 2021; Dhyani *et al*., 2022). In our previous studies, we reported on the potent anticancer activity of *Inula helenium* root extract and alantolactone isolated from the extract (Chun *et al*., 2015, 2018). Alantolactone has been shown to effectively suppress signal transducer and activator of transcription 3 (STAT3) activation, exhibiting significant anti-proliferative effects in MDA-MB-231 human breast cancer cells (Chun *et al*., 2015, 2018). Additionally, a range of sesquiterpene lactones, including alantolactone, costunolide, and parthenolide, have demonstrated STAT3 inhibitory activity across diverse contexts such as osteosarcoma, pancreatic cancer, cancer cachexia, and neuroinflammation (Zheng *et al*., 2019; Jin *et al*., 2020; Ding *et al*., 2022; Shen *et al*., 2022), reinforcing the potential of these natural compounds in targeting STAT3 (Youn *et al*., 2014; Formisano *et al*., 2017; Li *et al*., 2020; Dhyani *et al*., 2022). Despite these advances, the structure-activity relationship of sesquiterpene lactones in STAT3 inhibition, which is crucial for developing natural product-based STAT3-inhibitory pharmacophores, still needs to be defined.

STAT3, characterized by its Src homology 2 (SH2) domain,

Open Access **https://doi.org/10.4062/biomolther.2023.210**

Received Dec 5, 2023 **Revised** Feb 15, 2024 **Accepted** Feb 23, 2024
Published Online Aug 2, 2024

***Corresponding Authors**
E-mail: minsoonoh@snu.ac.kr (Noh M), hyejinko@kist.re.kr (Ko H)
Tel: +82-2-880-2481 (Noh M), +82-33-650-3573 (Ko H)
Fax: +82-2-880-2482 (Noh M), +82-33-650-3529 (Ko H)

is a transcription factor that plays a pivotal role in the regulation of cell survival, differentiation, and apoptosis (Garg *et al*., 2020; Zou *et al*., 2020). However, aberrant and constitutive activation of STAT3 is a defining feature in the pathogenesis of numerous human cancers, particularly in malignancies such as breast cancer (occurring in over 40% of cases) and cervical cancer (Shukla *et al*., 2010; Banerjee and Resat, 2016). Consequently, targeting STAT3 activity has gained attention as a promising and practical approach in breast cancer therapy. The constitutive activation of STAT3 triggers a series of events that result in the uncontrolled expression of oncogenes, fueling the relentless progression of the disease (Banerjee and Resat, 2016). In the context of breast cancers, triple-negative breast cancer (TNBC) is particularly challenging to treat due to its lack of hormone receptors and HER2 expression, which precludes the use of receptor-targeted therapies. This has led to the exploring STAT3 as an alternative therapeutic target, given its significant role in TNBC (Yu *et al*., 2009; Qin *et al*., 2019; Bi *et al*., 2023). TNBC cell lines are known to exhibit more pronounced constitutive activation of STAT3 compared to luminal-type breast cancer cell lines, underscoring the potential therapeutic advantage of targeting STAT3 in TNBC (Ko *et al*., 2019; Xie *et al*., 2019; Kim *et al*., 2023b). To leverage this insight, we assessed the anti-proliferative effects of sesquiterpene lactones on both TNBC and luminal-type breast cancer cell lines. The MDA-MB-231 cell line, a representative TNBC cell line, was chosen to investigate STAT3 inhibitory activity and the structure-activity relationship of sesquiterpene lactones.

The activation of STAT3 in both normal and tumor cells depends heavily on the phosphorylation of tyrosine residues, and specially Tyr705 (Resetca *et al*., 2014; Tošić and Frank, 2021; Hua *et al*., 2022). STAT3, which is recruited from the cytosol, can bind phosphotyrosine residues on activated cell surface receptors through its SH2 domain with nanomolar affinity (Belo *et al*., 2019). Subsequently, STAT3 is phosphorylated on its own tyrosine residues either directly by the receptor or by receptor-associated Janus kinases (Resetca *et al*., 2014; Hu *et al*., 2021; Tolomeo and Cascio, 2021). This phosphorylation leads to homodimerization or heterodimerization with other STAT family members, which is mediated by reciprocal interactions between the SH2 domain and the phosphorylated tyrosine (Zhang *et al*., 2013). STAT3 dimers then rapidly translocate from the cytosol to the nucleus, where they bind to specific promoter sequences in target genes and modulate the transcription of genes — such as cyclins, c-Myc, survivin, Bcl-2, and Mcl-1, all of which are involved in cell growth and apoptosis (Tolomeo and Cascio, 2021). Thus, inhibiting the SH2 domain-mediated STAT3 activation and dimerization represents a robust strategy for counteracting its biological activity (Zhang *et al*., 2013; Resetca *et al*., 2014; Tošić and Frank, 2021; Hua *et al*., 2022).

This study profiled the anti-proliferative and STAT3 inhibitory effects of ten sesquiterpene lactones in human breast cancer cell lines. Additionally, we performed molecular modeling studies to elucidate the structure-activity relationship of these sesquiterpene lactones, particularly about their capacity to inhibit STAT3 activation.

MATERIALS AND METHODS

Chemicals and reagents

Dulbecco's modified Eagle's medium (DMEM), penicillin, streptomycin, fetal bovine serum (FBS), and bovine serum albumin (BSA) were obtained from GenDepot (Barker, TX, USA). Dulbecco's phosphate buffered saline (DPBS), and a protease inhibitor cocktail were purchased from Sigma Aldrich (St. Louis, MO, USA). The primary antibodies for p-STAT3 (Tyr705) and STAT3 were from Abcam (Cambridge, MA, USA). The primary antibody for β-actin and all secondary antibodies were from Santa Cruz Biotechnology (Santa Cruz, CA, USA).

Preparation of sesquiterpene lactones

Alantolactone, isoalantolactone, costunolide, dehydrocostus lactone, parthenolide, atractylenolide I, atractylenolide II, atractylenolide III, and sclareolide, were purchased from Tauto Biotech (Shanghai, China). Tulipalin A (α-methylene-γ-butyrolactone) was purchased from Santa Cruz Biotechnology.

Cell culture

MCF-7 and MDA-MB-231 human breast cancer cell lines were obtained from the Korean Cell Line Bank (Seoul, Korea). BT-549 human breast cancer cell line was obtained from the American Type Culture Collection (ATCC, Manassas, VA, USA). These cells were maintained in high-glucose DMEM, supplemented with 10% FBS, penicillin 100 U/mL, and streptomycin 100 μg/mL at 37°C in a humidified atmosphere containing 5% CO_2.

Cell viability assay

Cell viability was evaluated using Cell Counting Kit-8 (CCK-8, Dojindo, Kumamoto, Japan) following the manufacturer's instructions. Breast cancer cells were plated at a density of 2×10^4 cells/well at 96-well plates and exposed to sesquiterpene lactones for 48 and 72 h. Then, 2-(2-methoxy-4-nitrophenyl)-3-(4-nitrophenyl)-5-(2,4-disulfophenyl)-2H tetrazolium solution was added to each well, followed by a 1-h incubation. The absorbance was measured at a wavelength of 450 nm using a microplate reader (Molecular Devices, Sunnyvale, CA, USA). The 50% inhibition concentration (IC_{50}) values were calculated using the four-parameter logistic regression.

Preparation of whole cell and nuclear extracts

Whole cell extracts were prepared using a lysis buffer (20 mM HEPES, pH 7.6, 350 mM NaCl, 20% glycerol, 0.5 mM EDTA, 0.1 mM EGTA, 1% NP-40, 50 mM NaF, 0.1 mM DTT, 0.1 mM PMSF, protease inhibitor cocktail, and PhosSTOP phosphatase inhibitor cocktail) for 30 min on ice. The lysates were centrifuged at 15,000 rpm for 10 min at 4°C. Nuclear extracts were prepared using a lysis buffer (10 mM HEPES, pH 7.9, 10 mM KCl, 0.1 mM EDTA, 0.1 mM EGTA, 1mM DTT, 1mM PMSF, and protease inhibitor cocktail) for 15 min on ice. Then, 10% NP-40 was added and the mixtures were centrifuged at 15,000 rpm for 5 min at 4°C. The nuclear pellets were resuspended in nuclear extraction buffer (20 mM HEPES, pH 7.9, 400 mM NaCl, 1 mM EDTA, 1 mM EGTA, 1 mM DTT, 1 mM PMSF, and protease inhibitor cocktail) and centrifuged at 15,000 rpm for 10 min at 4°C. The concentration of proteins was determined by the Bradford reagent (Bio-Rad, Hercules, CA, USA).

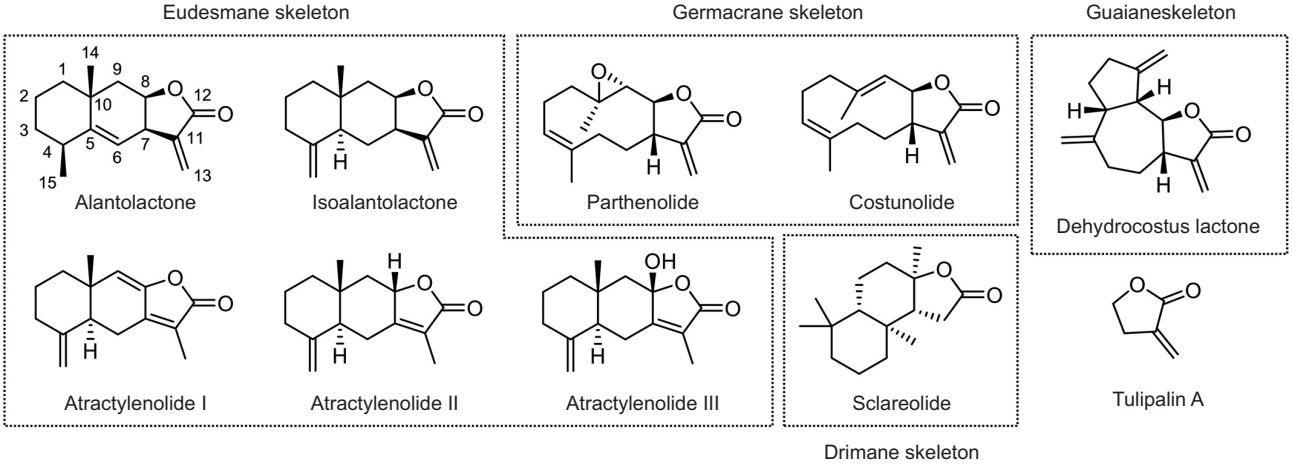

Fig. 1. Chemical structure of sesquiterpene lactones.

Western blotting

MDA-MB-231 cells were seeded into 6-well plates at a density of 4×10^5 cells/well. The cells were treated with sesquiterpene lactones for 4 h. Equal amounts of protein were separated on SDS-PAGE and transferred to nitrocellulose membranes. The membrane was blocked with 5% BSA, incubated with primary antibodies overnight, and incubated with secondary antibodies conjugated with HRP for 2 h. The immunoreactive bands were developed using a chemiluminescence kit (Intron Biotechnology, Seoul, Korea) and visualized using a LAS-1000 image analyzer (Fujifilm, Tokyo, Japan). Quantification of the western blot analysis was performed using ImageJ software (https://imagej.net/ij/) and the relative protein levels were normalized with those of vehicle control (Rueden *et al*., 2017).

Protein-ligand docking study

The three-dimensional (3D) coordinates of sesquiterpene lactones were generated and various conformers were searched using '--gen3d' and '--conformer' options of Open Babel v2.3.90 (https://openbabel.org/). We manually verified the absolute configurations, and geometry-optimized structures were obtained by conducting molecular mechanics simulation in Avogadro software v1.2.0 (https://avogadro.cc/) (Hanwell *et al*., 2012). To compare the 3D conformations, the 3D structures of sesquiterpene lactones were overlaid using '--align' option in Open Babel with the specified SMARTS pattern of γ-lactone. In molecular docking analysis, we utilized the X-ray crystal structure of pTyr705 STAT3 after extracting a monomer (PDB ID: 6QHD; Belo *et al*., 2019). Any missing residues were filled using the SWISS-MODEL server (Waterhouse *et al*., 2018). The docking site was defined as $30\times30\times30$ Å^3 grid box near the pTyr705 in the original crystal structure. We employed AutoDock Vina 1.1.2 software (https://vina.scripps.edu/) for the protein-ligand docking study as previously described (Trott and Olson, 2010; Kim *et al*., 2023a), and the top ten most energy-minimized binding modes were analyzed. For the analysis of protein-ligand interactions, the 'show_contacts' plugin was utilized in PyMOL (Schrodinger, Inc., New York, NY, USA).

Statistical analysis

All of the data are presented as the means ± standard deviations (SD) from at least three independent experiments. An analysis of variance (ANOVA) with the Dunnett's *t*-test was used for the statistical analysis of multiple comparisons. Pearson's correlation coefficient (R) was determined for the correlation analysis. A value of $p<0.05$ was considered to be statistically significant.

RESULTS

Anti-proliferative effects of sesquiterpene lactones in breast cancer cell lines

To investigate the structure-activity relationships of various sesquiterpene lactones in STAT3 activation, we selected ten representative sesquiterpene lactones characterized by their eudesmane (including alantolactone, isoalantolactone, atractylenolide I, atractylenolide II, and atractylenolide III), germacrane (parthenolide and costunolide), guaiane (dehydrocostus lactone), and drimane (sclareolide) skeletons (Fig. 1). In addition, we included tulipalin A, also known as α-methylene-γ-butyrolactone, for comparison because it shares a lactone ring with other sesquiterpene lactones.

We initially assessed the anti-proliferative effects of sesquiterpene lactones on human breast cancer cell lines, including MDA-MB-231, BT-549, and MCF-7 (Fig. 2). Cell viability was evaluated after treating the cells with various concentrations of sesquiterpene lactones for both 48 h and 72 h, from which IC_{50} values were derived. Notably, in MDA-MB-231 cells treated for 48 h, alantolactone (IC_{50}=13.3 μM), isoalantolactone (24.6 μM), parthenolide (13.7 μM), costunolide (27.1 μM), and dehydrocostus lactone (46.9 μM) exhibited dose-dependent anti-proliferative effects (Fig. 2A, 2B). In contrast, compounds such as atractylenolide I, atractylenolide II, atractylenolide III, sclareolide, and tulipalin A did not achieve more than 50% inhibition at the highest tested concentration of 50 μM, thus precluding the calculation of their IC_{50} values. In BT-549 cells, the anti-proliferative effects of alantolactone, isoalantolactone, parthenolide, costunolide, and dehydrocostus lactone were more potent than in MDA-MB-231 cells. Conversely, their ef-

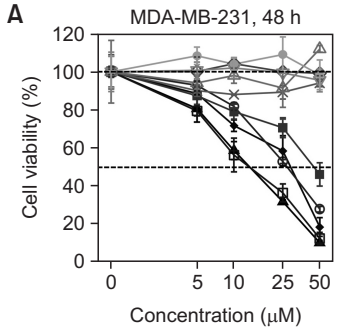

B

IC_{50} (μM)	TNBC				Luminal	
	MDA-MB-231		BT-549		MCF-7	
Time	48 h	72 h	48 h	72 h	48 h	72 h
Alantolactone	13.3±1.2**	9.9±0.7**	5.6±0.4**	4.5±1.1**	24.9±2.2	19.4±1.5
Isoalantolactone	24.6±1.8**	17.6±1.1**	17.1±2.5**	12.3±1.4**	39.6±3.6	38.3±2.5
Parthenolide	13.7±2.3*	10.6±3.3*	6.7±0.7**	6.0±0.5**	23.8±2.9	22.1±1.5
Costunolide	27.1±2.0*	20.3±1.5**	14.2±1.2**	12.6±1.0**	39.2±3.3	38.3±3.0
Dehydrocostus L.	46.9±1.8	23.2±1.0	17.1±2.4	7.9±1.6	N.D.	N.D.
Atractylenolide I	N.D.	N.D.	N.D.	N.D.	N.D.	N.D.
Atractylenolide II	N.D.	N.D.	N.D.	N.D.	N.D.	N.D.
Atractylenolide III	N.D.	N.D.	N.D.	N.D.	N.D.	N.D.
Sclareolide	N.D.	N.D.	N.D.	N.D.	N.D.	N.D.
Tulipalin A	N.D.	N.D.	N.D.	N.D.	N.D.	N.D.

Fig. 2. Anti-proliferative effects of sesquiterpene lactones in human breast cancer cell lines. (A) Anti-proliferative effects of sesquiterpene lactones in MDA-MB-231 cells after 48 h. (B) The IC_{50} values for anti-proliferative effects of sesquiterpene lactones in MDA-MB-231, BT-549, and MCF-7 cells. The cells were treated with varying concentrations of sesquiterpene lactones (ranging from 0 to 50 μM) for 48 h and 72 h, and the effects of sesquiterpene lactones on cell viability were measured. The results are presented as the mean ± SD of three independent experiments. *p<0.05 and **p<0.01 indicate the statistical significance compared to the IC_{50} value determined in MCF-7 cell line. N.D., not determined.

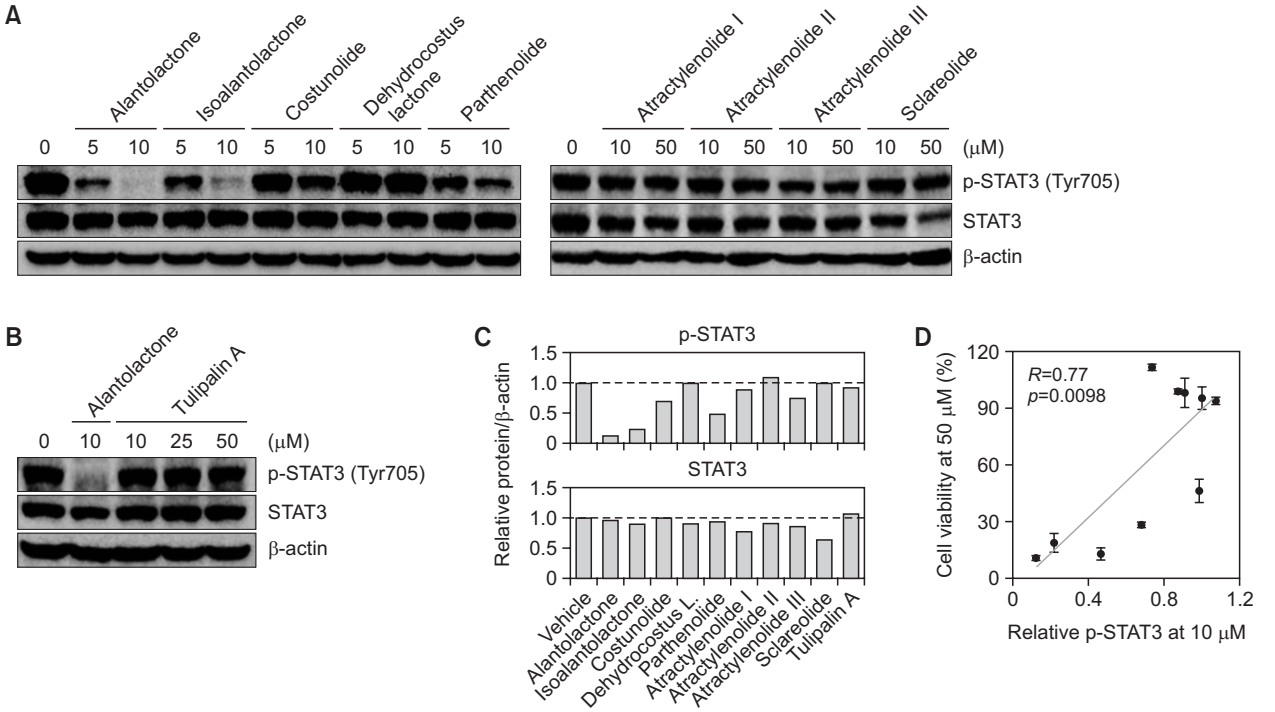

Fig. 3. Inhibitory effects of sesquiterpene lactones on STAT3 activation in MDA-MB-231 cells. (A, B) The cells were treated with sesquiterpene lactones for 4 h. Cell lysates were subjected to western blot analysis to determine the p-STAT3 (Tyr705) and STAT3 protein levels. β-actin was used as a loading control. (C) The western blot analysis quantified the levels of p-STAT3 and STAT3 proteins at 10 μM of sesquiterpene lactone. (D) Correlation analysis between relative p-STAT3 at 10 μM and 48-h anti-proliferative effects at 50 μM in MDA-MB-231 cells of sesquiterpene lactones.

fects in MCF-7 cells were significantly less potent (Fig. 2B). Consequently, IC_{50} values for the anti-proliferative effects were determined for only four sesquiterpene lactones, with dehydrocostus lactone excluded.

Inhibitory effect of sesquiterpene lactones on STAT3 activation in MDA-MB-231 cells

Next, we quantified the STAT3 inhibitory activity of sesquiterpene lactones to understand their structure-activity relationship. As illustrated in Fig. 3, the three out of ten sesquiterpene lactones — alantolactone, isoalantolactone, and parthenolide — effectively repressed the constitutive activation of STAT3, and specifically its phosphorylation of Tyr705 residue, without affecting the expression of total STAT3 proteins (Fig. 3A-3C). Costunolide and actractylenolide III exhibited mild inhibitory effects on p-STAT3, whereas the others had no impact on p-STAT3. Among the sesquiterpene lactones tested, alantolactone and isoalantolactone demonstrated the most potent inhibitory activities. Notably, we observed a significant correlation (R=0.77, p<0.01) between their inhibitory effects on

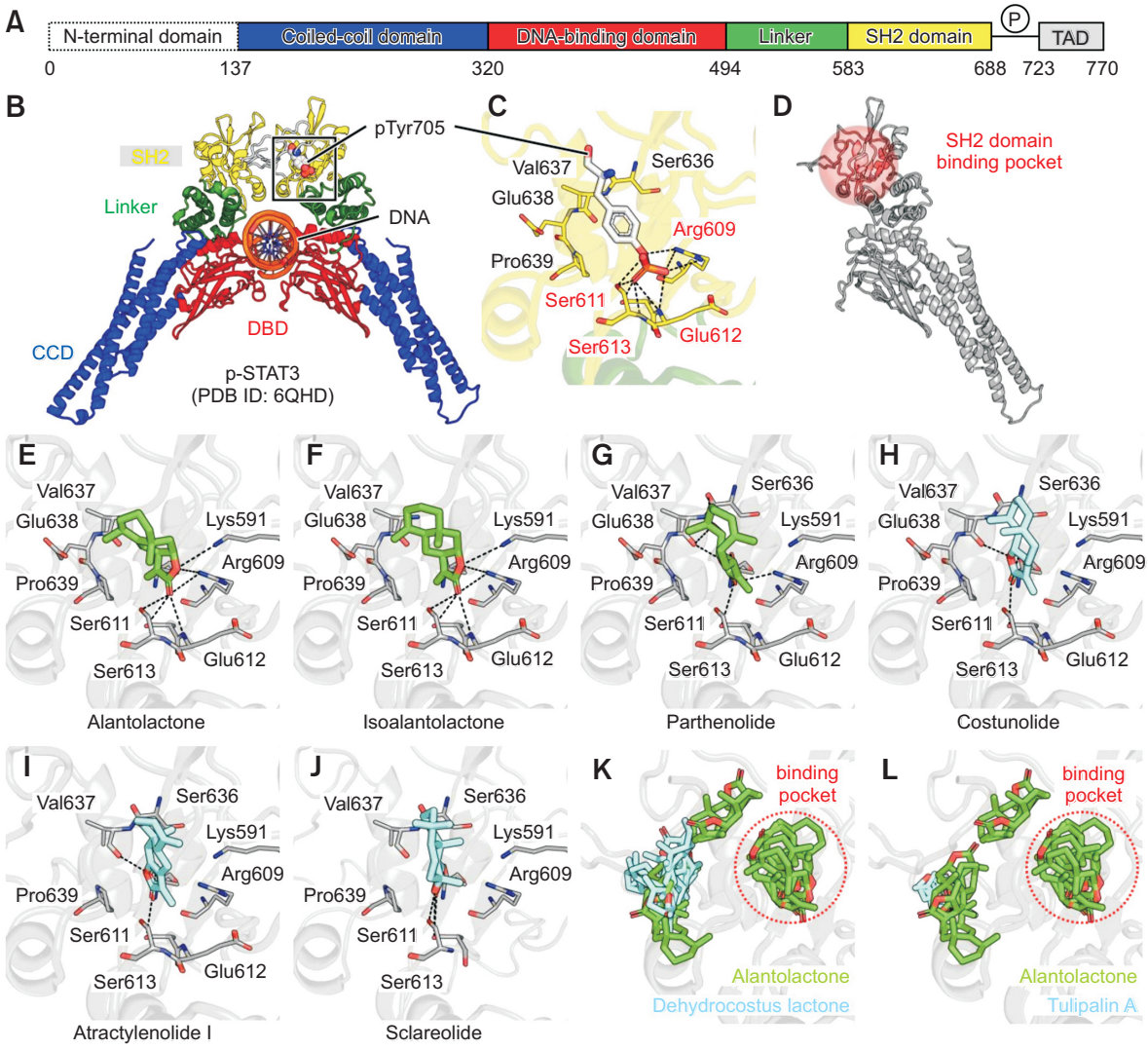

Fig. 4. Protein-ligand docking study of sesquiterpene lactones in STAT3. (A) Domain structured of STAT3. SH2, Src homology 2; TAD, transactivation domain. (B) X-ray crystal structure of p-STAT3 homodimer. (C) Key interacting amino acid residues of pTyr705 in SH2 domain binding pocket. Hydrogen bonds were shown in black dashes. (D) The location of SH2 domain binding pocket. Selected docking poses of sesquiterpene lactones; (E) alantolactone, (F) isoalantolactone, (G) parthenolide, (H) costunolide, (I) atractylenoide I, and (J) sclareolide. Top ten most energy-minimized binding modes of (K) dehydrocostus lactone, and (L) tulipalin A were compared with those of alantolactone.

STAT3 activation and their anti-proliferative effects (Fig. 3D), which strongly suggests that sesquiterpene lactones hinder the proliferation of MDA-MB-231 cells by modulating STAT3 phosphorylation.

Structural basis of STAT3 inhibition of sesquiterpene lactones

Despite their shared structural frameworks, sesquiterpene lactones exhibit notably different levels of STAT3 inhibition and anti-proliferative activities. Therefore, we performed a protein-ligand docking study to explore the structural basis of sesquiterpene lactones interact with STAT3 protein. STAT3 initiates downstream signaling by forming dimers through interactions between the SH2 domain of one monomer and the phosphorylated tyrosine residues of the other (Resetca *et al*., 2014). Several compounds interfering with this process have been identified as STAT3 inhibitors (Debnath *et al*., 2012; Ren *et al*., 2021). By analyzing the X-ray crystal structure of the STAT3 homodimer, whose dimerization is mediated by the pTyr705-SH2 interaction (Fig. 4A, 4B), we identified the key amino acid residues interacting between pTyr705 and the SH2 domain (Fig. 4C). We found that pTyr705 forms a hydrogen-bonding network with Arg609, Ser611, Glu612, and Ser613 in the SH2 domain of STAT3 (Shao *et al*., 2004). Consequently, the centroid of pTyr705 was designated as the docking site (Fig. 4D).

Alantolactone and isoalantolactone, identified as the most potent STAT3 inhibitors, engage in hydrogen-bonding interactions with specific residues — including Arg609, Ser611, Glu612, Ser613, and Lys591 — through their lactone rings (Fig. 4E, 4F). These interactions may competitively inhibit

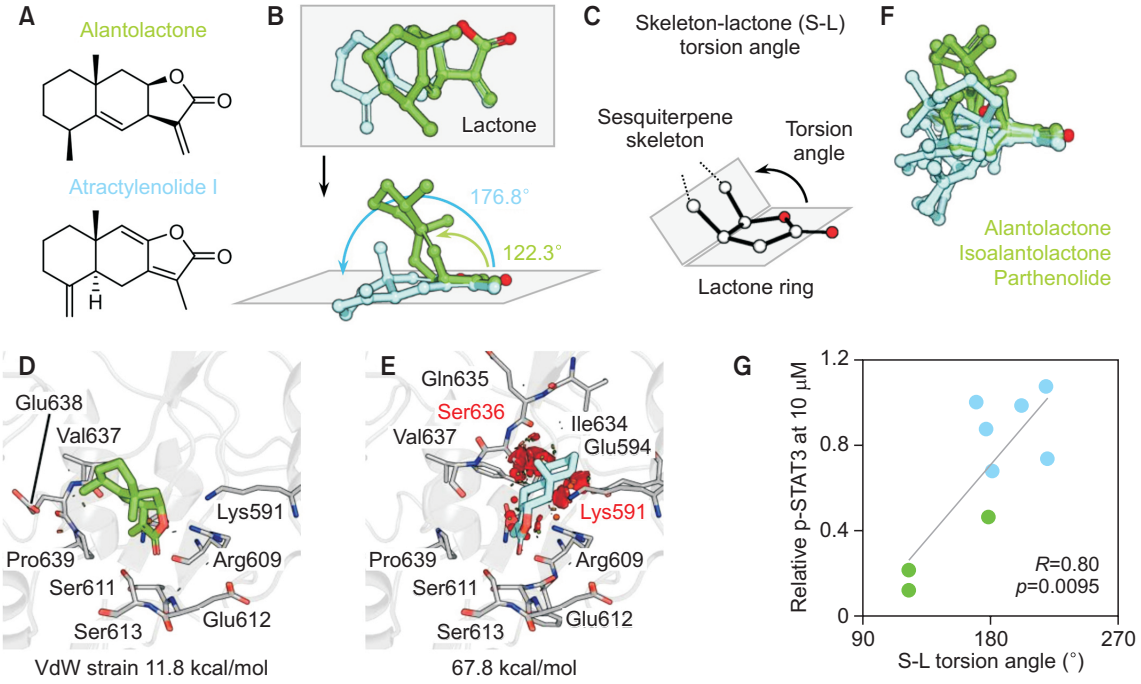

Fig. 5. Conformational analysis of sesquiterpene lactones. (A) 2D chemical structures of alantolactone and atractylenolide I. (B) Geometry optimized 3D structures of alantolactone (green) and atractylenolide I (cyan) were aligned based on their lactone rings. (C) Schematic diagram for determining the torsion angle between sesquiterpene skeleton-lactone ring (S-L torsion angle). We calculated Van der Waals (VdW) strains in SH2 binding pocket for alantolactone (D) and atractylenolide I (E). Putative VdW strains were visualized as red flat cylinders. (F) Geometry optimized 3D structures of sesquiterpene lactones were aligned based on their lactone rings. Sesquiterpene lactones, namely alantolactone, isoalantolactone, and parthenolide, which demonstrated over 50% inhibitory effects on STAT3 activation, are shown in green. (G) Correlation between S-L torsion angles and relative p-STAT3 at 10 μM of nine sesquiterpene lactones.

STAT3 dimerization through pTyr705. Parthenolide, which also exhibited STAT3 inhibitory and potent anti-proliferative activities, formed hydrogen bonds with Arg609 and Ser611 (Fig. 4G). The structural distinction between the potent parthenolide and the inactive costunolide lies in the double bond and the oxide moiety. Parthenolide formed hydrogen bonds through its oxide and amide carbonyl groups between the Val637 and Glu638 residues. Conversely, costunolide lacked these additional hydrogen bonds and was unable to form hydrogen bonds with Arg609 (Fig. 4G, 4H).

Actractylenolides display a structural difference at the C-8 position; specifically, the C-8 hydrogen of atractylenolide II is oxidized to a C-8 hydroxyl group, resulting in atractylenolide III, which transforms into atractylenolide I upon dehydration (Kim *et al*., 2018). Because this structural difference does not significantly affect STAT3 inhibition (Fig. 3C), we selected atractylenolide I among the actractylenolides to analyze the docking pose in the STAT3 SH2 domain. Notably, actractylenolide I and sclareolide, which showed low STAT3 inhibition activity, shared a protein-ligand interaction pattern similar to that of costunolide (Fig. 4I, 4J). Dehydrocostus lactone, with its bulkier seven-membered ring (instead of the six-membered ring in other sesquiterpene lactones), could not access the pTyr705 binding pocket (Fig. 4K). Tulipalin A, characterized by a smaller molecular structure, may exhibit a lower STAT3 inhibition potency because of nonspecific binding outside the binding pocket (Fig. 4L).

Critical stereochemical features of sesquiterpene lactones in STAT3 inhibition

Despite sharing the eudesmane skeleton, (iso)alantolactone and atractylenolides exhibited substantial differences in STAT3 inhibitory and anti-proliferative activities (Fig. 5A). Therefore, we performed a conformational analysis of these sesquiterpene lactones to uncover the structural basis behind these variations, using the geometry-optimized 3D conformations of sesquiterpene lactones. When these two compounds were aligned based on their lactone ring, which is crucial for binding to the STAT3 SH2 domain, we observed a significant difference in the orientation of their sesquiterpene skeletons (Fig. 5B). To quantitatively assess their conformational disparities, we determined the torsion angle between the sesquiterpene skeleton and lactone ring (S-L torsion angle) for each sesquiterpene lactone, as depicted in Fig. 5C. Notably, the S-L torsion angles were 122.3° for alantolactone and 176.8° for atractylenolide I (Fig. 5B). When comparing the binding mode in which the lactone ring aligns within the pTyr705 binding pocket, we noted Van der Waals (VdW) strains of 11.8 kcal/mol for alantolactone and 67.8 kcal/mol for atractylenolide I (Fig. 5D, 5E). In essence, in a scenario where the lactone ring interacts with Arg609, Ser611, and Ser613, a 3D conformation similar to that of atractylenolide I appears to disrupt the optimal interaction and binding of these compounds to the SH2 domain owing to significant steric repulsion with Lys591 and Ser636 residues (Fig. 5E).

When we compared the 3D conformations of all other sesquiterpene lactones and aligned them based on the lactone

rings, it became evident that the S-L torsion angles between compounds with STAT3 inhibitory activity and those with no effect were markedly different (Fig. 5F). Furthermore, the S-L torsion angles exhibited a significant and strong correlation (R=0.80, p<0.01) with the STAT3 inhibitory activity (Fig. 5G). These findings underscore the critical role of the stereochemistry and geometry-optimized 3D conformation in the development of anti-proliferative sesquiterpene lactones that target STAT3 phosphorylation.

DISCUSSION

Aberrant STAT3 activation is frequently observed in various human diseases, including breast and cervical cancers (Shukla *et al*., 2010; Banerjee and Resat, 2016). Many studies have suggested that STAT3 is a potential molecular target for the treatment and prevention of TNBC, which is both more aggressive and more difficult to treat because of the absence of receptors commonly found in other types of breast cancer (Qin *et al*., 2019; Bi *et al*., 2023). Therefore, the discovery of new potent and selective agents that can suppress STAT3 activation may be a promising approach for the treatment of breast cancer.

Sesquiterpene lactones constitute a significant group of natural products with a wide range of biological activities. Among these, their potent inhibitory effect on STAT3 has been observed in various cancer models, including osteosarcoma, breast and pancreatic cancer, and conditions like cancer cachexia (Chun *et al*., 2015, 2018; Zheng *et al*., 2019; Jin *et al*., 2020; Ding *et al*., 2022). Despite the established impact of sesquiterpene lactones on STAT3 activation, it remains to be fully elucidated. Alantolactone, in particular, has been noted for its pronounced inhibitory effect on STAT3 activation, underscoring its therapeutic promise in TNBC (Chun *et al*., 2015). Elevated levels of STAT3 phosphorylation have been documented in TNBC cell lines such as MDA-MB-231, BT-549, and BT-20, contrasting with low levels in luminal breast cancer cell lines like MCF-7 and T-47D (Ko *et al*., 2019; Xie *et al*., 2019; Kim *et al*., 2023b). This distinction has led to the selection of the MDA-MB-231 cell line as a suitable model for exploring the structure-activity relationship of sesquiterpene lactones in STAT3 inhibitory activity.

This study revealed that sesquiterpene lactones, including alantolactone, isoalantolactone, parthenolide, and costunolide, exert significant anti-proliferative effects in human breast cancer cell lines, notably in MDA-MB-231 and BT-549. In contrast, their effects were somewhat diminished in the luminal MCF-7 cell line, with IC_{50} values ranging between 19.4 to 39.6 μM, as opposed to the more pronounced effects observed in TNBC cell lines MDA-MB-231 and BT-549, which exhibited IC_{50} values between 9.9 to 27.1 μM and 4.5 to 17.1 μM, respectively. These findings highlight the critical role of aberrant STAT3 activation in the anti-proliferative activity of sesquiterpene lactones. Moreover, the strong correlation (R=0.77) between the inhibition of STAT3 activity and the reduction in cell proliferation further illustrates the essential function of STAT3 phosphorylation in regulating cellular growth.

This study further illuminated the structural foundation of STAT3 inhibition mediated by sesquiterpene lactones through comprehensive molecular modeling analyses. Protein-ligand docking study revealed that the most effective STAT3 inhibitors, namely alantolactone and isoalantolactone, establish hydrogen bonds with crucial amino acid residues within the SH2 domain of STAT3, including Arg609, Ser611, Glu612, and Ser613. Such interactions will likely interfere with STAT3 dimerization, a critical process for activating downstream signaling pathways. Moreover, our analysis highlighted the significance of the torsion angles between the lactone ring and the sesquiterpene backbone in determining the inhibitory potency of sesquiterpene lactones against STAT3. These findings contribute to a more nuanced understanding of the molecular mechanisms of sesquiterpene lactone-mediated STAT3 inhibition, and lay the groundwork for the structure-based development of new compounds with improved efficacy in inhibiting STAT3.

In conclusion, this study highlighted the potential of sesquiterpene lactones as promising candidates for targeting STAT3 in cancers involving constitutive STAT3 activation. Furthermore, structural insights gained through protein-ligand docking studies will pave the way for the development of novel compounds optimized for STAT3 inhibitory activity.

CONFLICT OF INTEREST

The authors have no conflicts of interest to declare.

ACKNOWLEDGMENTS

This study was supported by the National Research Foundation (NRF) of Korea (NRF-2022M3A9B6017654 and NRF-2020R1C1C1004573). H.K. is supported by the 'National Research Council of Science & Technology (NST)'-'Korea Institute of Science and Technology (KIST)' Postdoctoral Fellowship Program for Young Scientists at KIST in Republic of Korea.

REFERENCES

Banerjee, K. and Resat, H. (2016) Constitutive activation of STAT3 in breast cancer cells: a review. *Int. J. Cancer* **138**, 2570-2578.

Belo, Y., Mielko, Z., Nudelman, H., Afek, A., Ben-David, O., Shahar, A., Zarivach, R., Gordan, R. and Arbely, E. (2019) Unexpected implications of STAT3 acetylation revealed by genetic encoding of acetyl-lysine. *Biochim. Biophys. Acta Gen. Subj.* **1863**, 1343-1350.

Bi, J., Wu, Z., Zhang, X., Zeng, T., Dai, W., Qiu, N., Xu, M., Qiao, Y., Ke, L., Zhao, J., Cao, X., Lin, Q., Chen, X. L., Xie, L., Ouyang, Z., Guo, J., Zheng, L., Ma, C., Guo, S., Chen, K., Mo, W., Fu, G., Zhao, T. J. and Wang, H. R. (2023) TMEM25 inhibits monomeric EGFR-mediated STAT3 activation in basal state to suppress triple-negative breast cancer progression. *Nat. Commun.* **14**, 2342.

Chun, J., Li, R. J., Cheng, M. S. and Kim, Y. S. (2015) Alantolactone selectively suppresses STAT3 activation and exhibits potent anticancer activity in MDA-MB-231 cells. *Cancer Lett.* **357**, 393-403.

Chun, J., Song, K. and Kim, Y. S. (2018) Sesquiterpene lactones-enriched fraction of Inula helenium L. induces apoptosis through inhibition of signal transducers and activators of transcription 3 signaling pathway in MDA-MB-231 breast cancer cells. *Phytother. Res.* **32**, 2501-2509.

Debnath, B., Xu, S. and Neamati, N. (2012) Small molecule inhibitors of signal transducer and activator of transcription 3 (Stat3) protein. *J. Med. Chem.* **55**, 6645-6668.

Dhyani, P., Sati, P., Sharma, E., Attri, D. C., Bahukhandi, A., Tynybekov, B., Szopa, A., Sharifi-Rad, J., Calina, D., Suleria, H. A. R. and Cho, W. C. (2022) Sesquiterpenoid lactones as potential anti-

cancer agents: an update on molecular mechanisms and recent studies. *Cancer Cell Int.* **22**, 305.
Ding, W., Cai, C., Zhu, X., Wang, J. and Jiang, Q. (2022) Parthenolide ameliorates neurological deficits and neuroinflammation in mice with traumatic brain injury by suppressing STAT3/NF-κB and inflammasome activation. *Int. Immunopharmacol.* **108**, 108913.
Formisano, C., Sanna, C., Ballero, M., Chianese, G., Sirignano, C., Rigano, D., Millán, E., Muñoz, E. and Taglialatela-Scafati, O. (2017) Anti-inflammatory sesquiterpene lactones from Onopordum illyricum L. (Asteraceae), an Italian medicinal plant. *Fitoterapia* **116**, 61-65.
Garg, M., Shanmugam, M. K., Bhardwaj, V., Goel, A., Gupta, R., Sharma, A., Baligar, P., Kumar, A. P., Goh, B. C., Wang, L. and Sethi, G. (2020) The pleiotropic role of transcription factor STAT3 in oncogenesis and its targeting through natural products for cancer prevention and therapy. *Med. Res. Rev.* **41**, 1291-1336.
Hanwell, M. D., Curtis, D. E., Lonie, D. C., Vandermeersch, T., Zurek, E. and Hutchison, G. R. (2012) Avogadro: an advanced semantic chemical editor, visualization, and analysis platform. *J. Cheminform.* **4**, 17.
Hristozov, D., Da Costa, F. B. and Gasteiger, J. (2007) Sesquiterpene lactones-based classification of the family asteraceae using neural networks and k-nearest neighbors. *J. Chem. Inf. Model.* **47**, 9-19.
Hu, X., Li, J., Fu, M., Zhao, X. and Wang, W. (2021) The JAK/STAT signaling pathway: from bench to clinic. *Signal Transduct. Target. Ther.* **6**, 402.
Hua, Y., Yuan, X., Shen, Y. H., Wang, J., Azeem, W., Yang, S., Gade, A., Lellahi, S. M., Øyan, A. M., Ke, X., Zhang, W. D. and Kalland, K. H. (2022) Novel STAT3 inhibitors targeting STAT3 dimerization by binding to the STAT3 SH2 domain. *Front. Pharmacol.* **13**, 836724.
Jin, X., Wang, C. and Wang, L. (2020) Costunolide inhibits osteosarcoma growth and metastasis via suppressing STAT3 signal pathway. *Biomed. Pharmacother.* **121**, 109659.
Kim, D., Kim, J., An, S., Kim, M., Baek, K., Kang, B. M., Maharjan, S., Kim, S., Hwang, S. Y., Park, I. G., Park, S., Suh, J. G., Park, M. S., Noh, M., Lee, Y. and Kwon, H. J. (2023) *In vitro* and *in vivo* suppression of SARS-CoV-2 replication by a modified, short, cell-penetrating peptide targeting the C-terminal domain of the viral spike protein. *J. Med. Virol.* **95**, e28626.
Kim, J. H., Lee, Y., Lee, G., Doh, E. J. and Hong, S. (2018) Quantitative interrelation between atractylenolide I, II, and III in Atractylodes japonica Koidzumi rhizomes, and evaluation of their oxidative transformation using a biomimetic kinetic model. *ACS Omega* **3**, 14833-14840.
Kim, J. H., Park, S., Jung, E., Shin, J., Kim, Y. J., Kim, J. Y., Sessler, J. L., Seo, J. H. and Kim, J. S. (2023) A dual-action niclosamide-based prodrug that targets cancer stem cells and inhibits TNBC metastasis. *Proc. Natl. Acad. Sci. U. S. A.* **120**, e2304081120.
Ko, H., Lee, J. H., Kim, H. S., Kim, T., Han, Y. T., Suh, Y. G., Chun, J., Kim, Y. S. and Ahn, K. S. (2019) Novel galiellalactone analogues can target STAT3 phosphorylation and cause apoptosis in triple-negative breast cancer. *Biomolecules* **9**, 170.
Li, Q., Wang, Z., Xie, Y. and Hu, H. (2020) Antitumor activity and mechanism of costunolide and dehydrocostus lactone: two natural sesquiterpene lactones from the Asteraceae family. *Biomed. Pharmacother.* **125**, 109955.
Matos, M. S., Anastácio, J. D. and Nunes Dos Santos, C. (2021) Sesquiterpene lactones: promising natural compounds to fight inflammation. *Pharmaceutics* **13**, 991.
Qin, J. J., Yan, L., Zhang, J. and Zhang, W. D. (2019) STAT3 as a potential therapeutic target in triple negative breast cancer: a systematic review. *J. Exp. Clin. Cancer Res.* **38**, 195.
Ren, Y., Li, S., Zhu, R., Wan, C., Song, D., Zhu, J., Cai, G., Long, S., Kong, L. and Yu, W. (2021) Discovery of STAT3 and histone deacetylase (HDAC) dual-pathway inhibitors for the treatment of solid cancer. *J. Med. Chem.* **64**, 7468-7482.
Resetca, D., Haftchenary, S., Gunning, P. T. and Wilson, D. J. (2014) Changes in signal transducer and activator of transcription 3 (STAT3) dynamics induced by complexation with pharmacological inhibitors of Src homology 2 (SH2) domain dimerization. *J. Biol. Chem.* **289**, 32538-32547.
Rueden, C. T., Schindelin, J., Hiner, M. C., DeZonia, B. E., Walter, A. E., Arena, E. T. and Eliceiri, K. W. (2017) ImageJ2: ImageJ for the next generation of scientific image data. *BMC Bioinformatics* **18**, 529.
Shao, H., Xu, X., Mastrangelo, M. A., Jing, N., Cook, R. G., Legge, G. B. and Tweardy, D. J. (2004) Structural requirements for signal transducer and activator of transcription 3 binding to phosphotyrosine ligands containing the YXXQ motif. *J. Biol. Chem.* **279**, 18967-18973.
Shen, Q., Kuang, J. X., Miao, C. X., Zhang, W. L., Li, Y. W., Zhang, X. W. and Liu, X. (2022) Alantolactone ameliorates cancer cachexia-associated muscle atrophy mainly by inhibiting the STAT3 signaling pathway. *Phytomedicine* **95**, 153858.
Shukla, S., Shishodia, G., Mahata, S., Hedau, S., Pandey, A., Bhambhani, S., Batra, S., Basir, S. F., Das, B. C. and Bharti, A. C. (2010) Aberrant expression and constitutive activation of STAT3 in cervical carcinogenesis: implications in high-risk human papillomavirus infection. *Mol. Cancer* **9**, 282.
Shulha, O. and Zidorn, C. (2019) Sesquiterpene lactones and their precursors as chemosystematic markers in the tribe Cichorieae of the Asteraceae revisited: an update (2008-2017). *Phytochemistry* **163**, 149-177.
Tolomeo, M. and Cascio, A. (2021) The multifaced role of STAT3 in cancer and Its implication for anticancer therapy. *Int. J. Mol. Sci.* **22**, 603.
Tošić, I. and Frank, D. A. (2021) STAT3 as a mediator of oncogenic cellular metabolism: pathogenic and therapeutic implications. *Neoplasia* **23**, 1167-1178.
Trott, O. and Olson, A. J. (2010) AutoDock Vina: improving the speed and accuracy of docking with a new scoring function, efficient optimization, and multithreading. *J. Comput. Chem.* **31**, 455-461.
Waterhouse, A., Bertoni, M., Bienert, S., Studer, G., Tauriello, G., Gumienny, R., Heer, F. T., de Beer, T. A. P., Rempfer, C., Bordoli, L., Lepore, R. and Schwede, T. (2018) SWISS-MODEL: homology modelling of protein structures and complexes. *Nucleic Acids Res.* **46**, W296-W303.
Xie, Q., Yang, Z., Huang, X., Zhang, Z., Li, J., Ju, J., Zhang, H. and Ma, J. (2019) Ilamycin C induces apoptosis and inhibits migration and invasion in triple-negative breast cancer by suppressing IL-6/STAT3 pathway. *J. Hematol. Oncol.* **12**, 60.
Youn, U. J., Miklossy, G., Chai, X., Wongwiwatthananukit, S., Toyama, O., Songsak, T., Turkson, J. and Chang, L. C. (2014) Bioactive sesquiterpene lactones and other compounds isolated from Vernonia cinerea. *Fitoterapia* **93**, 194-200.
Yu, H., Pardoll, D. and Jove, R. (2009) STATs in cancer inflammation and immunity: a leading role for STAT3. *Nat. Rev. Cancer* **9**, 798-809.
Zhang, X., Sun, Y., Pireddu, R., Yang, H., Urlam, M. K., Lawrence, H. R., Guida, W. C., Lawrence, N. J. and Sebti, S. M. (2013) A novel inhibitor of STAT3 homodimerization selectively suppresses STAT3 activity and malignant transformation. *Cancer Res.* **73**, 1922-1933.
Zheng, H., Yang, L., Kang, Y., Chen, M., Lin, S., Xiang, Y., Li, C., Dai, X., Huang, X., Liang, G. and Zhao, C. (2019) Alantolactone sensitizes human pancreatic cancer cells to EGFR inhibitors through the inhibition of STAT3 signaling. *Mol. Carcinog.* **58**, 565-576.
Zou, S., Tong, Q., Liu, B., Huang, W., Tian, Y. and Fu, X. (2020) Targeting STAT3 in cancer immunotherapy. *Mol. Cancer.* **19**, 145.